International Journal of Multidisciplinary and Current Research ISSN: 2321-3124
Research Article Available at: http://ijmcr.com

Numerical Study of Coupling Effect on the Optical Properties of Two Assembled Gold Nanorods Coated with Stimuli-Responsive Polymers

A. Akouibaa[*] M.Benhamou[#], Z. Bassam[*], A. Derouiche[*], and S. El-fassi[*]

[*]Polymer Physics and Critical Phenomena Laboratory. Hassan II University Casablanca, Sciences Faculty Ben M.sik, P.O. Box 7955, Casablanca, Morocco.
[#]ENSAM, Moulay Ismaïl University, Meknès, Morocco.

Accepted 01 June 2016, Available online 11 June 2016, **Vol.4 (May/June 2016 issue)**

Abstract

Grafting stimuli-responsive polymers to gold nanorods (GNRs) is a convenient way to render them responsive to changes in environmental conditions such as pH and temperature. With a water-soluble polymer ligand tethered to the surface of GNRs, a stable dispersion in water can be obtained. Recent studies found that if the polymer chains become insoluble due to either a temperature change or a pH change, aggregation of GNRs can occur, resulting in a reduced optical transmittance of the solution and a shift of the surface plasmon resonance (SPR) mainly as a result of closer distances between the surfaces of GNRs. In this paper a model based on the finite element method (FEM) is developed to investigate the optical properties of GNRs dimer coated with stimuli-responsive polymeric shells. The study is performed for various possible configurations of two core/shell GNRs when they are aggregating in dielectric medium, to know; the side-to-side (parallel-shape) and end-to-end association. The numerical results that we have obtained show that the absorption spectrum of assembled GNRs is depending on the: polymer shell thickness, its dielectric permittivity and aspect ratio of the gold core nanorods.

Keywords: *Gold nanorods, core/shell nanostructures, optical properties, finite element.*

1. Introduction

Gold nanorods (GNRs) with distinctive shape-dependent optical properties have drawn worldwide attention in the biomedical field. These nanorods possess two different plasmon bands, one is the transverse plasmon band in the visible region at around $520\ nm$, and the other is the longitudinal plasmon band in the near-infrared region. These unique properties make gold nanorods excellent materials for biological sensing, imaging, photothermal therapy, drug delivery, and other biological applications [1-4]. However, there are several problems that influence and limit the application of gold nanorods. A small change in the size, shape, local environment, surface nature, and degree of aggregation of nanorods will lead to tunable changes in their properties, which in turn affect their applications [5].

Gold nanorods (GNRs), which are rod-shaped gold nanoparticles (GNPs), show high promising potential as light-triggered, remotely controlled molecular release trigger in response to optical excitation. The plasmon resonance of GNRs can be tuned from the visible to NIR regions that depend on the nanorod's aspect ratio [6]. The NIR laser irradiation-triggered drug and gene release is especially attractive, because GNRs can be easily made to maximally absorb in the "water window" [7]. In addition, GNRs have the advantages of efficient large-scale synthesis and can be easily decorated with multiple molecular species to simultaneously provide biological compatibility, [8,9] activated drug and gene delivery [10,11] and direct cell specific targeting [12,3]. In view of the importance of gold nanoparticles (GNPs) in many emerging applications such as sensing, delivery, and cancer therapy, [14] developing new stimuli responsive GNPs is of interest. To our knowledge, all thermo-sensitive polymer-coated GNPs reported thus far display a lower critical solution temperature (LCST), meaning that the polymer becomes insoluble in water when solution temperature is raised to $T > LCST$. To make polymer-coated GNPs respond to temperature change in the opposite way, *i.e*. with a polymer that becomes insoluble in water upon lowering temperature, the coated polymer should exhibit an upper critical solution temperature (UCST).

Kumacheva *et al.*[15,16] developed a strategy for inducing the self-assembly of nanorods by functionalizing them with hydrophobic ligands (such as polystyrene, octadecylphosphonic acid, or hexylphosphonic acid), followed by adding polar solvents (water or DMF) into nanorod dispersions in non-polar organic solutions

(toluene) to reduce the solubility of the surface ligands, thus causing their attraction to form assemblies of attached nanorods in an end-to-end [15] manner. A side-by-side [16] assembly of Au-tipped CdSe nanorods has also been achieved by applying this approach.

Manna *et al*.[17] demonstrated a self-assembly approach for nanorods employing depletion attraction, defined as[18] an effective attractive force that arises between large colloidal particles that are suspended in a dilute solution of depletants, which are smaller solutes that are preferentially excluded from the vicinity of the large particles. The assembly was triggered by adding additives such as long alkyl chain fatty acids and amines, the liquid crystal 4'-n-pentyl-4-cyanobiphenyl (5CB), oleic acid, or polymers (polystyrene, polyethylene glycol methacrylate) into the nanorod dispersions in organic solvents to form close-packed hexagonally ordered monolayer arrays. The exclusion of the additives from between the nanorods resulted in a local concentration gradient, which led to the close packing of the nanorods.

It is well-known that the plasmon resonance of metal nanoparticles is strongly sensitive to the nanoparticle size, shape, and the dielectric properties of the surrounding medium. Optical properties of gold nanoparticles can thus be readily tuned by varying their size and shape.[19-21] In addition, Halas and *co-workers* [25] have shown that the use of composite nanoparticles based on a core-shell morphology (e.g., silica-gold nanoshells) allows optical tunability by variation in the composition.

There have been several experimental reports [22] on the optical properties of metal nanoparticles, including gold nanospheres [20,21], nanorods,[23], bimetallic nanoparticles,[24] composite nanoparticles with a core-shell structure,[25] and nanoparticle chains and assemblies.[26,27]. At the same time, well-established theoretical tools based on the Mie theory [28] , the discrete dipole approximation (DDA) [29] method and the finite element method (FEM) [30,31] have been readily exploited for a quantitative study of the nanoparticle optical properties of different size, shape, composition, and aggregation state, etc.[32,33]. In this paper, we use the FEM method to calculate the absorption cross section and optical resonance wavelengths of dimer gold-core/polymer-shell nanorods, for different arrangements in space, these configurations result from the orientation of the electric applied field relative to the nanorods orientation, so as to aid the selection of nanoparticles morphology for specific biomedical applications. Our approach is implemented in the framework of quasi-static approximation. For this we will limit our study to a binary gold nanorod coated with stimuli-responsive polymers. The optical response of two assembled gold-core/polymer-shell nanorods depends on their orientations one relative to each other, namely the assembly end-to-end or side-to-side. The effect of several geometrical and physical parameters including the polymer shell thickness, its dielectric permittivity and the nanorod aspect ratio on the absorption spectrum are analyzed and compared.

2. Methodology and Model.

2.1 Modeling of Gold Nanorods Coated with Polymers.

The creation of core/shell nanoparticles (CSNs) has in recent years developed into an increasingly important research area at the frontier of advanced materials chemistry.[34-37] The importance stems largely from the diverse attributes of CSNs as model building blocks towards functional materials, including 1) size monodispersity, 2) core and shell processibility, 3) solubility, 4) stability, 5) tunability, 6) capability of self-assembly, and 7) reactivities involving optical, electronic, magnetic, catalytic, and chemical/biological phenomena. Many types of nanoparticles could fit into the core/shell category, which is recently broadly defined [36] as core and shell of different matters in close interaction, including inorganic/organic, inorganic/inorganic, organic/organic, or inorganic/biological core/shell combinations.[34-38].

In our study, the core-shell model is employed to characterize the gold nanorods coated with stimuli-responsive polymers, in this model the gold core is represented by a nanorod which is enclosed by another representing the polymeric shell. The fitting geometrical parameters for this model are: the aspect ratio of the gold core that is defined by the quotient $\eta_c = h/r$ such that h is the nanorod height and r its radius and the polymer shell thickness e, the aspect ratio of the gold-core/polymer-shell nanoparticle is $\eta_p = H/r$ such that $H = h + 2e$ and $R = r + e$ this nanoparticle is Surrounded by an dielectric medium as shown in *Fig.1*. The physical parameter characterizing the different phases of the nanocomposite is the dielectric permittivity (gold core ε_c, polymer shell ε_p and surrounding medium ε_m).

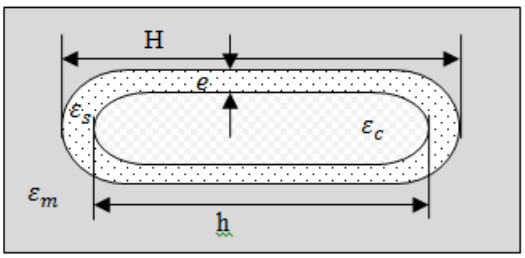

Fig.1 Representation of the core-shell nanorod model

The dielectric constant of gold core is a function of electromagnetic wave frequency with which it interacts. Indeed, the interaction of the electromagnetic wave defined by its pulsation ω, with a metal lead to polarization of the medium. This polarization then generates a change in the complex refractive index, $\tilde{n}(\omega)$ which is related to the dielectric constant by the following relationship: $\tilde{n}^2(\omega) = \varepsilon(\omega)$.

2.2 Dielectric Permittivity of Noble Metal

The frequency-dependent electric permittivity is an important parameter to be known in advance when studying the frequency response of the material over a wide frequency range. Traditionally, Drude-Lorentz (DL) model which can well represent the optical properties of the metal originating from the interband and intraband transitions was the popular one and has been used to quantify the dispersion properties of the metal [39,40]. In DL model, a large number of Lorentz oscillators can be used to model the line shape of the electric permittivity of the material over the frequency range of interest [41]. However, the accuracy improvement obtained via adding more Lorentz terms comes with a price. A large number of Lorentz terms lead to increased requirement of computational resources such as CPU power and memory [42].

Recently, Drude-critical point (DCP) model that consists of one Drude term and two critical point terms was proposed which can satisfactorily represent the electric permittivity of metals over a wide frequency range [41-43]. From the computational perspective, DCP model is advantageous over DL model since the former requires only less number of terms. Since then, DCP model has been used to represent the electric permittivity of metals such as gold and others with good accuracy [44].

The DCP dispersive model expresses interband transitions featuring asymmetric line shapes with critical point terms instead of Lorentzian terms [41]. The relative electric permittivity as per the DCP model can be written

$$\varepsilon_r(\omega) = \varepsilon_\infty + \chi_D(\omega) + \sum_{p=1}^{2} \chi_p(\omega) \quad (1)$$

Where ε_∞ is the relative electric permittivity at infinite frequency, $\chi_D(\omega)$ the Drude susceptibility, and $\chi_p(\omega)$ the critical point susceptibility. The Drude susceptibility is expressed as:

$$\chi_D(\omega) = -\frac{\omega_D^2}{\omega^2 + i\gamma\omega} \quad (2)$$

Where ω_D is the Drude pole frequency and γ the inverse of the pole relaxation time. Also, the critical point susceptibility is expressed as:

$$\chi_p(\omega) = A_p\Omega_p\left(\frac{e^{i\phi_p}}{\Omega_p - \omega - i\Gamma_p} + \frac{e^{-i\phi_p}}{\Omega_p + \omega + i\Gamma_p}\right) \quad (3)$$

Where A_p is the amplitude, ϕ_p the phase, $\hbar\Omega_p$ the energy gap, and Γ_p the broadening.

2.3 Numerical Method

In this work we are interested in determining the effective dielectric permittivity of nanocomposite constituted by dimer GNRs coated with polymers immersed in a dielectric medium using the Finite Element FE numerical tool. The detailed description of the method for determining the effective permittivity in the quasi-static limit can be found elsewhere [45]. As both computing power and the efficiency of the FE computational method, it is becoming possible to investigate new composite materials through computer simulations before they have even been synthesized. FE tool is used to compute the solution of Laplace equation by determining the electric field and potential distribution from the physical properties of different phases of the composite material. Recent works have shown that the FE method could be successfully applied to compute the effective permittivity of periodic composite materials (e.g. [46]. The basic scheme of the FE method is now briefly recalled.

To describe the FEM scheme, we consider a spatial domain, Ω, contains two nanorods shown in *Fig.2* with a vanishing charge density. Solving the problem at hand means finding the local potential distribution inside the computational domain by solving Laplace's equation (first principal of electrostatic):

$$\vec{\nabla}\left(\varepsilon_0\varepsilon(\vec{r})\vec{\nabla}V(\vec{r})\right) = 0\,, \quad (4)$$

Where $\varepsilon(r)$ and $V(\vec{r})$ are the local relative permittivity and the potential distribution inside the material domain respectively with zero charge density $\varepsilon_0 = 8.85.10^{-12}$SI is the permittivity of the vacuum. In addition, the composite (dielectric) is assumed to be periodic with three phases (metallic core, polymeric shell and host matrix). Taking into account the symmetry and periodicity properties, the geometry of the medium is reduced to a unit cell. The implementation of the FE method consists in dividing the three-dimensional domain into tetrahedral finite elements and interpolating the potential V and its normal derivative $\frac{\partial V}{\partial n}$ on each finite element similarly to the BIE method [47,48] with the corresponding nodal values:

$$V = \sum_i \lambda_i V_i \quad (5)$$

$$\frac{\partial V}{\partial n} = \sum_i \lambda_i \left(\frac{\partial V_i}{\partial n}\right) \quad (6)$$

Where λ_i denotes the interpolating functions.

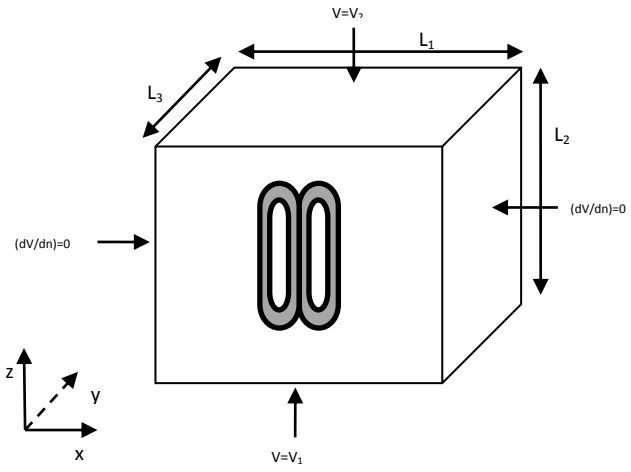

Fig.2 Notation and boundary conditions related to a three-dimensional periodic nanocomposite. This cell contains two coupled coated gold nanorods

Following this analysis, the solution of Laplace's equation is obtained using the Galerkin method and by solving the resulting matrix equation from the boundary conditions thanks to a standard numerical technique, *i.e*., Gauss procedure [4].

Having computed the potential and its normal derivative on each tetrahedron of the computational mesh, the electrostatic energy W_e^k, and losses, P_e^k could be expressed for each tetrahedral element as:

$$W_e^k = \frac{\varepsilon_0}{2}\iiint_{V_k} \varepsilon_k^{'}(x,y,z)\left[\left(\frac{\partial V}{\partial x}\right)^2+\left(\frac{\partial V}{\partial y}\right)^2+\left(\frac{\partial V}{\partial z}\right)^2\right]dV_k\,, \quad (7)$$

$$P_e^k = \frac{\varepsilon_0}{2}\iiint_{V_k} \omega\varepsilon_k^{''}(x,y,z)\left[\left(\frac{\partial V}{\partial x}\right)^2+\left(\frac{\partial V}{\partial y}\right)^2+\left(\frac{\partial V}{\partial z}\right)^2\right]dV_k\,,. \quad (8)$$

Where ε_k and V_k represent the permittivity and the volume of the k^{th} tetrahedron element, respectively. Thus, the total energy and losses in the entire composite can be written by summation over the n_k elements such as:

$$W_e = \sum_{k=1}^{n_k} W_e^k \quad (9)$$

$$P_e = \sum_{k=1}^{n_k} P_e^k \quad (10)$$

To compute quantities W_e and P_e, we suppose that the composite material is embedded in a plane capacitor. This way allows us to determine the effective permittivity in a direction parallel to the applied electric field. Then, from the capacitor electrostatic energy expression, we deduce the effective (complex) permittivity. We find that the real part,$\varepsilon_{eff}^{'}$, and imaginary one, $\varepsilon_{eff}^{''}$, parallel to the applied electric field, are given by:

$$W_e = \frac{1}{2}\varepsilon_{eff}^{'}\frac{S_d}{L_3}(V_2-V_1)^2\,, \quad (11)$$

$$P_e = \frac{1}{2}\omega\varepsilon_{eff}^{''}\frac{S_d}{L_3}(V_2-V_1)^2\,. \quad (12)$$

Where V_1 and $V_2$are the potentials applied across to plates of the unit cell (Fig. 2). Here, $S_d = L_1.L_3$ is the surface of in-depth. The real and imaginary parts of the effective permittivity then depends on the total energy, W_e , losses, P_e , linear size L_2 and applied potential difference $V_2 - V_1$. In addition, the second one is frequency-dependent. If the amplitude of the applied field is equal to 1, so the potential difference is kept equal to $\Delta V = L_2$. The following paragraph will be devoted to the determination of the optical properties of the material under investigation.

2.4 Absorption-cross-section

From the evolution of the effective complex dielectric function depending on the wavelength (or frequency) of the incident field, the resonance modes that may occur in nanoparticles are identified. For this, it would be interesting to calculate the scattering cross-sections and absorption. The sum of these two quantities defines the extinction cross-section

$$\sigma_{ext} = \sigma_{abs} + \sigma_{diff}. \quad (13)$$

In the case where the dimensions are very small compared to the wavelength, the light scattering can be ignored, and we have: $\sigma_{ext} \approx \sigma_{abs}$.

The cross-section of extinction (absorption) can be determined from the imaginary part of the effective dielectric function of the composite using the following equation [50].

$$\sigma_{abs} = \frac{V_p}{f}\frac{k}{n_{eff}}\varepsilon_{eff}^{''}\,. \quad (14)$$

Here, V_p stands for the common volume of nanoparticles, f is their fraction, k is the wave-vector amplitude of the electromagnetic wave, and n_{eff} represents the refractive index that can be related to the real and imaginary parts, $\varepsilon_{eff}^{'}$ and $\varepsilon_{eff}^{''}$, of the effective permittivity by [51].

$$n_{eff} = \left(\frac{\sqrt{\varepsilon_{eff}^{'2}+\varepsilon_{eff}^{''2}}+\varepsilon_{eff}^{'}}{2}\right)^{1/2}. \quad (15)$$

This formula clearly shows that the peak of $\mathrm{Im}(\varepsilon_{eff})$ indicates that the light is rather absorbed in specific regions. The effective dielectric function and the effective refraction index are calculated using FEM. Hence, the section of optical absorption is easily obtained. In the following section, we present and discuss our findings.

3. Results and discussion

Gold nanorods exhibit transverse (T) and longitudinal (L) plasmon resonance modes that correspond to the electron oscillations which are perpendicular and parallel to the length axis of the nanorod, respectively. In this work we are interested in the study of the optical properties of two assembled gold nanorods coated with polymer shell using the FEM. For this nanocomposite system the variation of the conformation of polymers chains can lead to the formation of aggregates nanoparticles. In particular the conformation of polymer chain depends on several environmental stimuli such as the temperature, PH, Solvents, Electromagnetic radiation (UV, visible) and others. The *Fig.3* shows a schematic illustration of the assembly mechanism of the gold nanorods by the stimuli-responsive polymers intermediaries grafted on their surfaces. The stimuli collapse of polymer chains onto solid cores will decrease the spatial occupy and the surface property when the distance between two nanorods becomes very small the coupling effect exchange the interaction process of these nanoparticles with an incident electromagnetic wave which modifies the SPR properties of these nanoparticles.

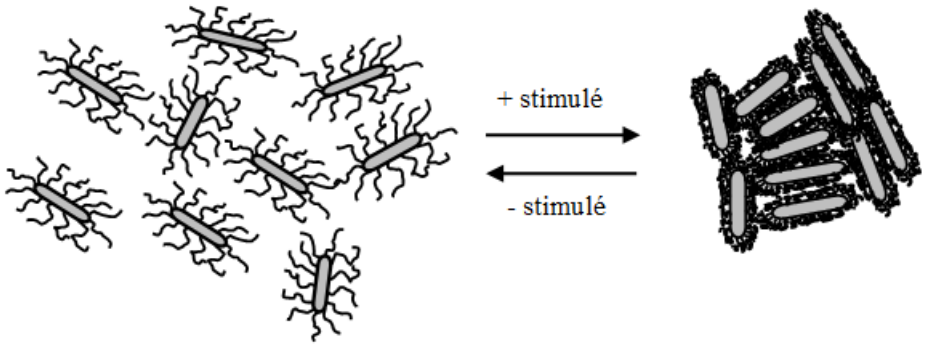

Fig.3 Schematic representation of the assembly of Gold nanorods by stimuli-responsive polymers

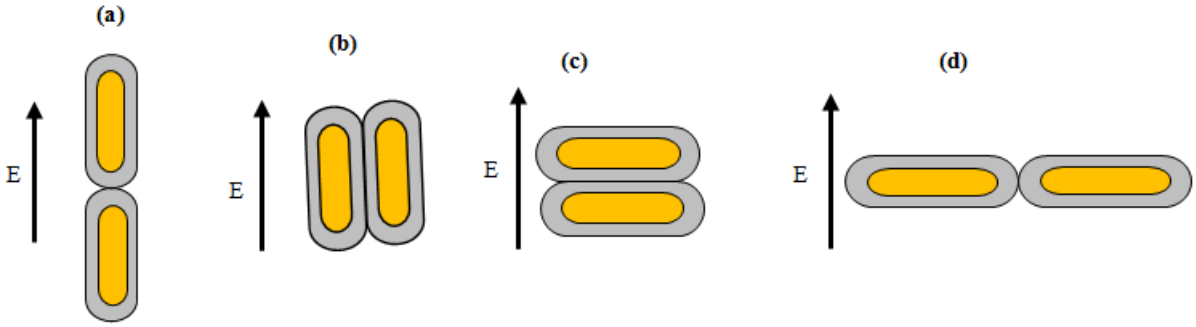

Fig.4 Schematic representation of various configurations of two assembled coated-GNRs: L-mode with end-to-end assembly (a), L-mode with side-to-side assembly (b), T-mode with side-to-side assembly(c) and T-mode with end-to-end assembly (d)

To respect the limits imposed by the quasi-static approximation used in this simulation we are limiting our study in the case of binary coated GNRs. For this, we consider two assembled GNRs with different configurations as shown in *Fig.4*, for these nanostructures the dependence of SPR on the shell thickness, permittivity of the polymer shell and gold-core aspect ratio will be discussed systematically. The optical response of two assembled coated GNRs depends on their Arrangement one relative to the other and their orientation relative to the electric field. When the field is applied parallel to the nanorods it's the longitudinal mode (L-mode) which will be excited, whereas when the field is perpendicular to the nanorods it is the transverse mode (T-mode) is excited.

3.1 End-to-end assembling

We consider two similar GNRs with chosen parameters: height $\mathrm{h} = 32\mathrm{nm}$ and diameter $\mathrm{d} = 8\mathrm{nm}$ the aspect ratio of this nanoparticle is $\eta = 4$, defined by the ratio of height to diameter, these two nanorods are superposed end-to-end parallel to direction of the applied electric field *(Fig.4a)* and are migrated into aqueous dielectric medium of permittivity ε_{m} with a volume fraction $\phi_{\mathrm{v}} = 0.05$. The polymer shell thickness noted e and dielectric permittivity ε_{p}, the total core/shell nanorod radius is $\mathrm{R} = \mathrm{r} + \mathrm{e}$ and its height is $\mathrm{H} = \mathrm{h} + 2\mathrm{e}$. For this configuration we examine the effect of the polymer shell thickness on the plasmonic properties in the case where the two nanorods are in contact and the effect of the interparticle distance when the two nanorods are separated by a distance d with fixed polymer shell thickness.

Fig.5a illustrate the variation of the absorption cross section depending on the electromagnetic wave energy for different values of the polymer shell thickness of two similar core/shell nanorods when they are in contact end-to-end with excitement of the longitudinal mode. These curves are obtained with the following fixed parameters: gold core radius $\mathrm{r} = 4\mathrm{nm}$ and height $\mathrm{h} = 28\mathrm{nm}$, the radius and the total height of the core/shell nanorods are respectively $\mathrm{R} = \mathrm{r} + \mathrm{e}$ and $\mathrm{h} = \mathrm{H} + 2\mathrm{e}$ with e is the polymer shell thickness, the volume fraction $\phi_{\mathrm{v}} = 0.05$ which is the ratio of the tow nanorods volume V_{ps} on the simulated cell volume V_c: $\phi_v = V_{ps}/\, V_c$ the permittivity of the surrounding medium $\varepsilon_{\mathrm{m}} = 1.77$ and those of the polymer shell $\varepsilon_{\mathrm{p}} = 3.4$ $(\varepsilon_{\mathrm{m}} < \varepsilon_{\mathrm{p}})$.

These curves show that when the polymer shell thickness increases the optical resonance peak moves toward the infrared wavelengths. When the variation of the polymer shell thickness, two effects taken into consideration: the coupling effect in the case of the smaller values of e that is a result of the Rapprochement of two gold core and the coating effect in the case of the large values of e for which the polymer layers becomes thicker i.e. the two cores move away relatively.

In order to explain the results shown in *Fig.5a*, we represent in *Fig.5b* the effect of the variation of e in the case where ($\varepsilon_p < \varepsilon_m$), $\varepsilon_p = 2.0$ and $\varepsilon_m = 2.25$ and we keep the others parameters unchanged. These curves show that the optical resonance peak moves to the infrared wavelength when the thickness e decreases. These results show that when $\varepsilon_m < \varepsilon_p$ the coating effect on the optical properties of two coated gold NRs dominates relative to the coupling effect, whereas when $\varepsilon_p < \varepsilon_m$ the coupling effect becomes more important compared to that coating effect.

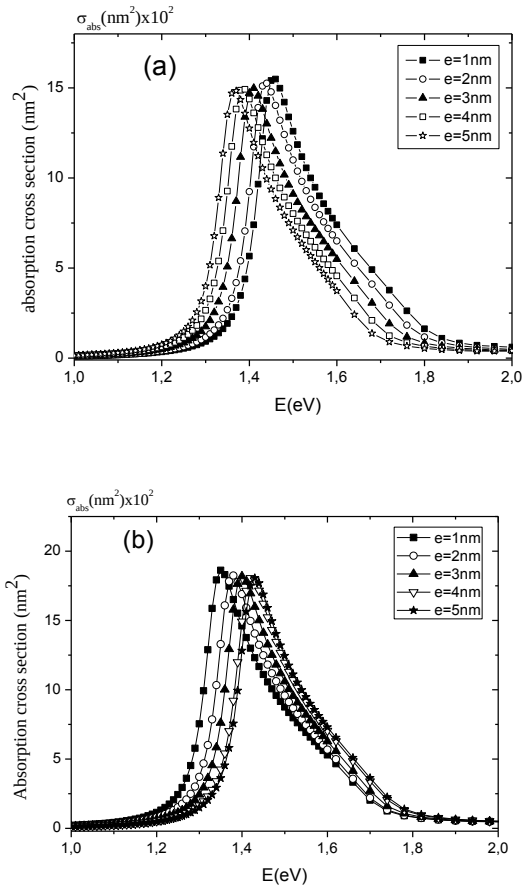

Fig.5a, 5b Evolution of the absorption cross section of two assembled (end-to-end) gold-core/polymer-shell nanorods upon photon energy for different values of polymer shell thicknesses , in the case of $\varepsilon_m < \varepsilon_p$ **5a** and $\varepsilon_m > \varepsilon_p$ **5b**.

Another important situation in the case of end-to-end assembling is when the two ends of the nanorods are separated by a distance d. To study the separation distance effect on the plasmonic properties, we fix the polymer shell thickness at $e = 2nm$ and we trace the absorptions spectra for different values of d. *Figs.6a, 6b* show the obtained results for two different values of ε_m and ε_p respectively $\varepsilon_m < \varepsilon_p$ ($\varepsilon_m = 1.77$, $\varepsilon_p = 3.4$) and $\varepsilon_p < \varepsilon_m$ ($\varepsilon_m = 2.25$, $\varepsilon_p = 2.0$). The curves in *Fig.6a* show that for $\varepsilon_m < \varepsilon_p$, the SPR peak position does not change when the interparticle distance decreases which shows that the optical response of core/shell nanorods is influenced only by the coating effect while the coupling effect is screened. Furthermore, the curves in Fig.6b show that for $\varepsilon_p < \varepsilon_m$ the position peak of the optical resonance moves toward infrared wavelengths when the separation distance decreases, in this case the effect coupling takes place which modify the optical response of the two assembled nanorods.

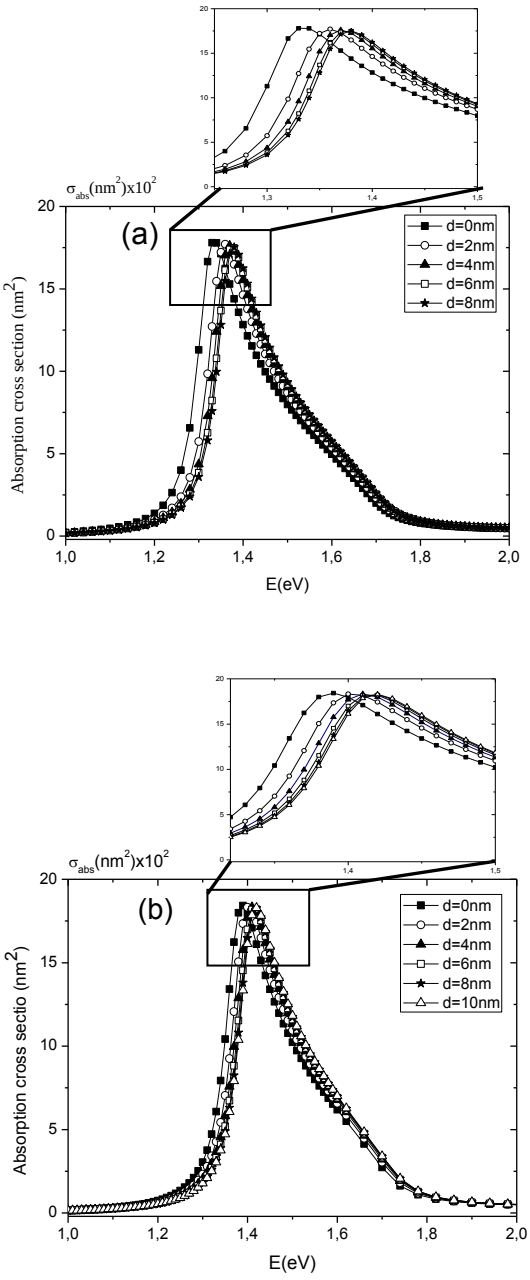

Fig.6a, 6b Evolution of the absorption cross section of two assembled (end-to-end) gold-core/polymer-shell nanorods upon photon energy for different values of interparticle separation distance , in the case of $\varepsilon_m < \varepsilon_p$ **6a** and $\varepsilon_m > \varepsilon_p$ **6b**.

3.2 Side-to-side assembling

Now consider two similar core-gold/ polymer-shell nanorods closer by their sides, this configuration called side-to-side assembling which is represented in *Fig 4b*. These nanorods are superposed parallel to the direction of the external electric field, that is to say we excite the longitudinal mode. In order to study their optical properties we suppose that these two nanorods are submerged in a dielectric medium that has a permittivity ε_m and a volume fraction ϕ_v. The geometrical and physical parameters of the dimer nanorods are noted as follows: gold-core radius r, height h, polymer shell thickness e, total radius and total height of the core/shell nanorods are respectively $R = r + e$ and $H = h + 2e$ and the polymer shell permittivity is noted by ε_p. For this configuration we examine the effect of the polymer shell thickness in the case where the two nanorods are in contact, and the effect of the separation distance when the two nanorods sides are separated by a distance d along with the fixed shell thickness.

Figs.7a-7b shows the variation of the absorption cross section function of photon energy for different values of the polymer shell thickness for two side-to-side assembled nanorods respectively for $\varepsilon_m < \varepsilon_p$ and $\varepsilon_m > \varepsilon_p$. These curves are obtained we choose the following parameters: gold core radius $r = 4nm$, height $h = 28nm$, volume fraction $\phi_v = 0.05$, polymer shell permittivity are $\varepsilon_p = 3.4$ for *Fig7a* and $\varepsilon_p = 2.0$ for *Fig.7b* and the surrounding medium permittivity are $\varepsilon_m = 1.77$ (*Fig.7a*) and $\varepsilon_m = 2.25$ (*Fig.7b*). These curves show that when the polymer shell thickness increases, the optical resonance peak moves toward the infrared wavelength, this shifting is very important in the case where $\varepsilon_m < \varepsilon_p$ (*Fig.7a*), while for $\varepsilon_m > \varepsilon_p$ (*Fig.7b*) this shift is small.

In order to model the displacement of the resonance peak in function of the shell thickness, we represent in *Fig.8* the variation of the wavelength λ_{max} corresponding to the resonance in function of the polymer shell thickness e, these curves show that λ_{max} varies almost linearly with the thickness e. Starting from these two curves we can model the wavelength corresponding to the resonance by the following linear functions $\lambda_{max} = 34.04e + 722.98(nm)$ in the case $\varepsilon_m < \varepsilon_p$ and $\lambda_{max} = 7.46e + 763.67(nm)$ in the case $\varepsilon_m > \varepsilon_p$. It is important to note that in the case $\varepsilon_m < \varepsilon_p$ the slope of the λ_{max} function is larger compared to that obtained in the case where $\varepsilon_m > \varepsilon_p$. It is important to note that in the case $\varepsilon_m < \varepsilon_p$ the slope of the $\lambda_{max}(e)$ function is larger compared to the obtained in the case where $\varepsilon_m > \varepsilon_p$.

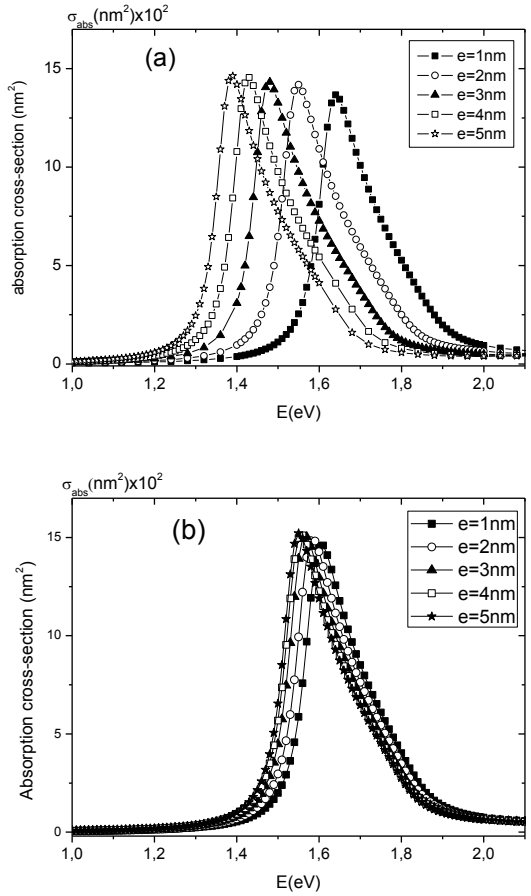

Fig.7a, 7b Evolution of the absorption cross section of two assembled (side-to-side) gold-core/polymer-shell nanorods upon photon energy for different values of polymer shell thicknesses *e* in the case of $\varepsilon_m < \varepsilon_p$ **7a** and $\varepsilon_m > \varepsilon_p$ **7b**.

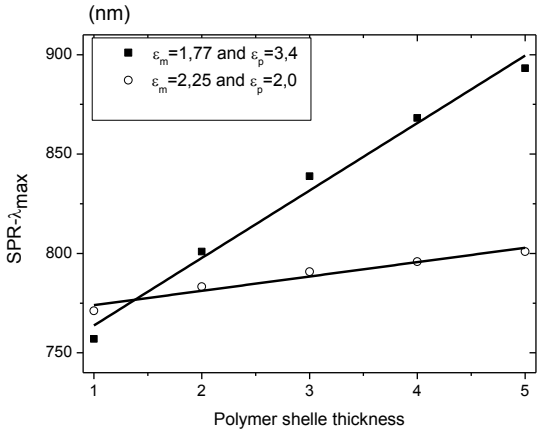

Fig.8 Evolution of the SPR_λ_{max} position upon polymer shell thickness of two assembled (side-to-side) gold-core/polymer-shell nanorods, in the cases of $\varepsilon_m < \varepsilon_p$ and $\varepsilon_m > \varepsilon_p$.

Now let us consider two gold-core/polymer-shell nanorods with the same previous geometrical and physicals parameters, the two nanorods are close together side-by-side and separated by a distance d. The aim here is to study the influence of the separation

distance on the plasmonic properties, for this we represent in *Figs.9a and 9b* respectively the absorption spectra within two different cases $\varepsilon_m < \varepsilon_p$ and $\varepsilon_m > \varepsilon_p$. These curves show that, when the two nanorods are closer (distance d decreases) the position of the resonance peak moves towards the visible wave length in the two cases whereas the amplitude absorption does not change. *Fig.10* shows the variation of the wavelength λ_{max} corresponding to the SPR in function to the interparticle distance for the two cases $\varepsilon_m < \varepsilon_p$ and $\varepsilon_m > \varepsilon_p$. These two curves show that for a fixed distance d, the resonance peak position is located near the infrared region in the case where $\varepsilon_m < \varepsilon_p$ compared to the case where $\varepsilon_m > \varepsilon_p$.

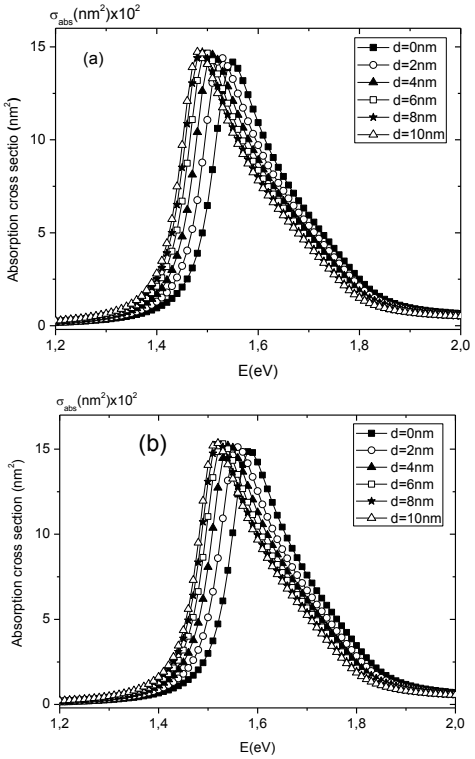

Fig.9a, 9b Evolution of the absorption cross section of two assembled (side-to-side) gold-core/polymer-shell nanorods upon photon energy for different values of interparticle separation distance , in the case of $\varepsilon_m < \varepsilon_p$ **9a** and $\varepsilon_m > \varepsilon_p$ **9b**.

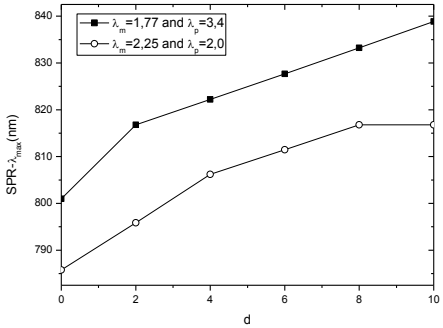

Fig.10 Evolution of the SPR_λ_{max} position upon interparticle separation distance of two assembled (side-to-side) gold-core/polymer-shell nanorods, in the cases of $\varepsilon_m < \varepsilon_p$ and $\varepsilon_m > \varepsilon_p$.

3.3 Effect of the polymer shell permittivity.

One of the parameters which can influence the optical response of gold-core/polymer-shell nanoparticles is the dielectric permittivity of the latter and that of the surrounding medium. Indeed, the permittivity of polymer layer coating metal nanoparticle depends on several parameters, for example the grafting density, solvent quality and the polymers nature. Several theoretical and experimental studies have been realized to investigate the effect of the permittivity of the surrounding medium on the optical properties of an isolated gold nanorod with and without coating [52,53]. These studies show that the variation of the wavelength corresponding to the optical resonance follows a linear equation in function of the surrounding medium permittivity. The aim in this section is to study the effect of the polymer-shell dielectric permittivity on the plasmonic properties of two gold-core/polymer-shell nanorods assembled end-to-end or side-to side

For this we consider two core/shell nanorods in contact by their ends or their sides, these two nanorods are disposed parallel to the applied electric field direction i.e. we excite the longitudinal mode. The physical and geometrical parameters of the system are chosen as follows: gold core radius $r = 4nm$, height $h = 32nm$, polymer shell thickness $e = 2nm$, total radius and total height of the core/shell nanorods are respectively $R = r + e = 6nm$ and $H = h + 2 = 36nm$, volume fraction $\phi_v = 0.05$ and the dielectric permittivity of surrounding medium is $\varepsilon_m = 1.77$. *Figs. 11a and 11b* shows the variation of the absorption cross section for different values of the polymer shell permittivity in function of photon energy respectively for the two assembling configuration end-to-end and side-to-side. These curves show that when the polymer dielectric permittivity increases the SPR peak position moves toward infrared wavelength for the two cases of assembling end-to-end and side-to-side.

In order to model the dependence of the optical resonance to the polymer shell permittivity ε_p, we represent in *Fig.12* the variation of the wavelength λ_{max} corresponding to the surface plasmons resonance in function of ε_p. This figure shows that λ_{max} varies linearly in function of ε_p with the following formulas $\lambda_{max} = 34.64\varepsilon_p + 746.42(nm)$ in the case of end-to-end assembling and $\lambda_{max} = 29.4\varepsilon_p + 697.57(nm)$ in the case of side-to-side assembling, from these relationships it is possible to predict the SPR peak position for other values of ε_p. On the other hand these curves show that for the same value of ε_p the wavelength λ_{max} corresponding to the optical resonance is located near infrared in the case of the end-to-end assembling unlike to the case of side-to-side assembling.

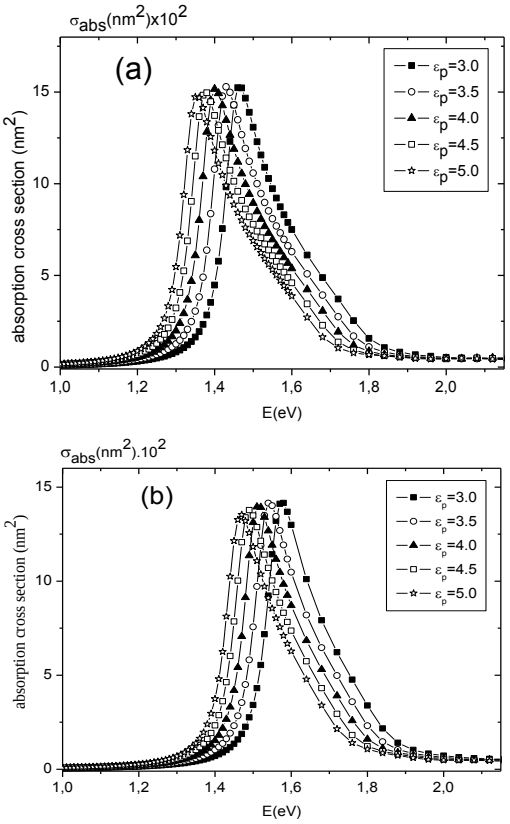

Fig.11a, 11b Evolution of the absorption cross section of two assembled gold-core/polymer-shell nanorods upon photon energy for different values of polymer shell permittivity for the assembling end-to-end (**11a**) and side-to-side (**11b**).

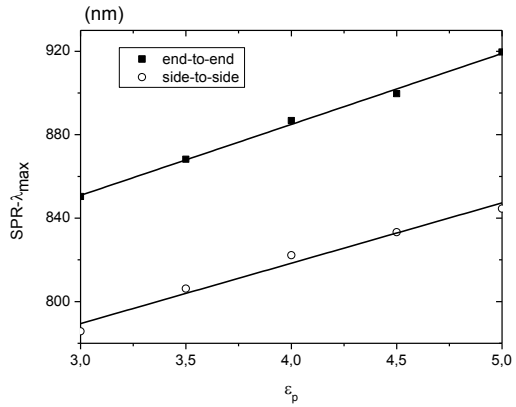

Fig.12 Evolution of the SPR_λ_{max} position upon polymer shell permittivity ε_p of two assembled gold-core/polymer-shell nanorods, in the cases of the assembling end-to-end and side-to-side.

3.4 effect of the aspect ratio.

One parameter that plays a crucial role in modeling the optical properties of the gold nanorods is the aspect ratio denoted η this parameter determines the nanoparticle geometry is defined as the ratio of the nanorod height on their diameter $\eta = h/2r$, with r is the nanorod radius. Several experimental and theoretical studies have been conducted on the effect of the aspect ratio on the spectral properties of the isolated gold nanorods with and without coating [53-56]. These studies showed that the wavelength corresponding to the plasmon resonance varies proportionally with the nanorod aspect ratio. In *Figs. 13a and 13b* we examine the effect of the aspect ratio on SPR properties of two assembled gold-core/shell polymer nanorods which are in contact respectively end-to-end or side-to-side. These curves are obtained for a fixed polymer shell thickness $e = 2\text{nm}$ and for different values of η.

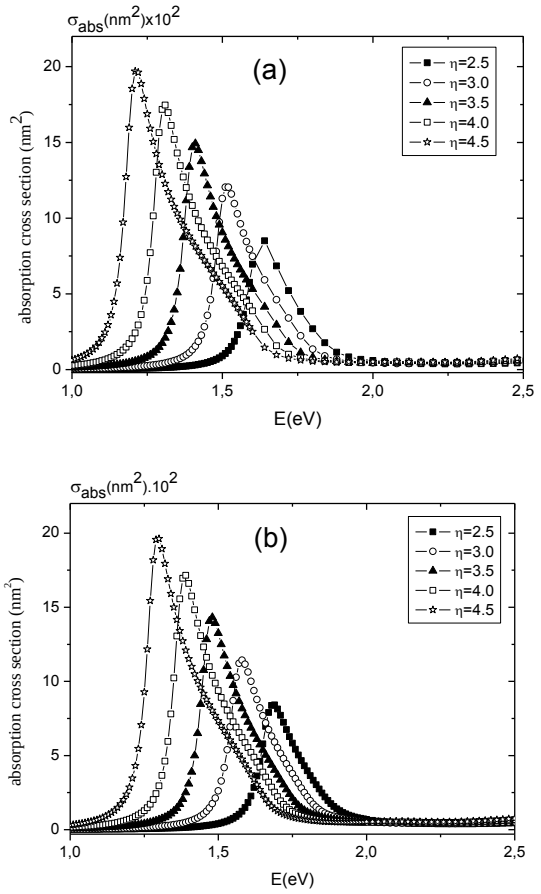

Fig.13a 13b Evolution of the absorption cross section of two assembled gold-core/polymer-shell nanorods upon photon energy for different values of gold core aspect ratio for the assembling end-to-end (**13a**) and side-to-side (**13b**).

The curves in *Fig.13a* show for the end-to-end assembling that when the aspect ratio varies from $\eta = 2.5$ to $\eta = 5$ the optical resonance peak moves towards the infrared from $\lambda_{\max} = 757.02\text{nm}$ to $\lambda_{\max} = 1098.69\text{nm}$, this displacement is accompanied by an increasing of the amplitude absorption. Whereas in the case of the side-to-side assembling Fig.13b shows that when the aspect ratio varies from $\eta = 2.5$ to $\eta = 4.5$ the optical resonance peak moves toward the infrared from $\lambda_{\max} = 734.63\text{nm}$ to $\lambda_{\max} = 955.02\text{nm}$. The shift of the optical resonance peak to the infrared wavelength follows a linear law in

two assembling cases end-to-end and side-to-side what is show in *Fig.14*. Using these curves we can pull the functions modeling the variation of $\lambda_{\max}$ in function of η, $\lambda_{\max} = 136.67\eta + 415.35\ (\mathrm{nm})$ for the end-to-end assembling and $\lambda_{\max} = 110.2\eta + 459.14\ (\mathrm{nm})$ for side-to-side assembling, starting from the last we can predict the SPR peak position for another value of η.

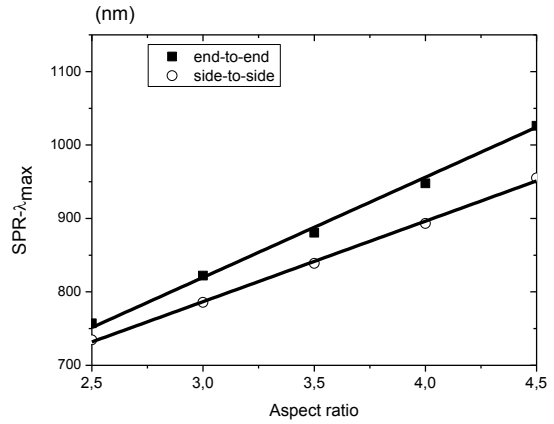

Fig.14 Evolution of the SPR_λ_{max} position upon gold core aspect ratio η of two assembled gold-core/polymer-shell nanorods, in the cases of the assembling end-to-end and side-to-side

Conclusions

This work has been devoted to study the optical properties of assembled gold nanorods via the stimuli-responsive polymers grafted on their surface.

For this we used the core/shell model, the core represents the gold kernel and the shell is the polymer coating layer, the dielectric permittivity of gold core is determined from the two critical points Drude model. The optical properties of gold nanoparticles immersed in a dielectric medium are quantified by the effective dielectric permittivity of nanocomposite (matrix-nanoparticles).

The important phenomenon intervening when the interacting between electromagnetic wave and gold nanoparticles is the surface plasmon resonance (SPR), this phenomenon is the basis of extraordinary optical properties of gold nanoparticles and who is due to the collective oscillation of surface electron. The major problems that arise when using gold nanoparticles in biology are: the stabilization, biocompatibility, self assembly of nanoparticles and their functionalization. For pull up these problems, the specialists frequently use the macromolecules and polymers to coat the gold nanoparticles. One category of polymers used in this context is the stimuli-responsive polymers that changes conformation following a change of an external stimuli. This conformation change leads to the polymer chains collapse and we witness to aggregation (assembly) of gold nanoparticles, or polymer chain swelling which leads to the dispersion of nanoparticles in dielectric medium. When two gold-core/polymer-shell nanorods approach each other, several configurations can create: end-to-end assembly when the two nanorods approach by their ends, side-by-side assembly when the two nanorods approach by their sides or angular assembly when the two nanorods form an angle between them. In this work we studied the two assemblies' cases, end-to-end and side-to-side when the electric field is applied parallel to the nanorods axis this situation called longitudinal mode excitation.

We have established a series of 3D-simulations using FEM to determining the optical properties of two assembled GNRs with various configuration, which are embedded in a host dielectric medium. More precisely, we have computed the effective permittivity of these nanostructures this parameter has allowed us to calculate the absorption cross section of these nanoparticles.

In a first step we have studied the effect of polymer shell thickness on the plasmonic properties of two assembled gold-core/polymer-shell nanorods when they are in contact end-to-end or side-to-side, and the effect of the separation distance when they are separated by a distance d. For the end-to-end assembly the obtained results show that, when the shell thickness decreases the optical resonance peak moves toward the visible region in the case where $\varepsilon_{\mathrm{m}} < \varepsilon_{\mathrm{p}}$ and toward the infrared in the case where $\varepsilon_{\mathrm{p}} < \varepsilon_{\mathrm{m}}$, such as ε_{m} and ε_{p} are respectively, the dielectric permittivity of the medium surrounding and of the polymer shell. For the same configuration (end to end) we have studied also the effect of the interparticle distance when the two nanorods are separated by a distance d. The obtained results show that when the distance d decreases, the surface plasmon resonance peak moves slightly toward the infrared wavelength in the two cases $\varepsilon_{\mathrm{m}} < \varepsilon_{\mathrm{p}}$ and $\varepsilon_{\mathrm{p}} < \varepsilon_{\mathrm{m}}$. For the side-to-side assembling the obtained results show that when the shell thickness decreases, the optical resonance peak moves towards the visible wavelength in two cases $\varepsilon_{\mathrm{m}} < \varepsilon_{\mathrm{p}}$ and $\varepsilon_{\mathrm{p}} < \varepsilon_{\mathrm{m}}$, this displacement is very pronounce for $\varepsilon_{\mathrm{m}} < \varepsilon_{\mathrm{p}}$. For this side-to-side configuration with a separation distance d. the obtained absorption spectra show that when the interparticle distance decreases the optical resonance peak position moves towards the visible in the two cases $\varepsilon_{\mathrm{m}} < \varepsilon_{\mathrm{p}}$ and $\varepsilon_{\mathrm{p}} < \varepsilon_{\mathrm{m}}$.

Thereafter, we have studied the effect of polymer shell dielectric permittivity ε_{p} on the plasmonic properties of two gold-core/shell-polymer assembled nanorods The obtained results show that the wavelength corresponding to the optical resonance $\lambda_{\max}$ is linearly varies according to ε_{p} with the following equation $\lambda_{\max} = \mathrm{a}\varepsilon_{\mathrm{p}} + \mathrm{b}(\mathrm{nm})$ in the two arrangement types end-to-end and side-to-side, such a the director coefficient a and the constant b depending the dielectric constant of surrounding medium ε_{m} and the volume fraction of inclusions. Firstly, this relation shows that when ε_{p} increases the resonance peak position moves toward the infrared region, secondly starting from this relationship we can predict the resonance peak position for any value of ε_{p}.

Finally, we have studied the effect of the aspect ratio of gold core, for this we draw the absorption spectra of two gold-core/shell polymer assembled nanorods end-to-end or side-to-side for different values of aspect ratio. The obtained results show that for the two assembly types, when the aspect ratio increases the SPR peak position moves toward infrared. This shift follows a linear law depending the aspect ratio, which is modeled by the following equation $\lambda_{\max} = a'\eta + b' \,(\mathrm{nm})$, such as the constants a' and b' take different values depending on the arrangement type end-to-end or side-to-side.

References

[1]. D.P. Yang and D.X. Cui, (2008) Advances and prospects of gold nanorods, *Chem Asian J.*,3, pp.2010-2022.

[2]. J. Stone, S. Jackson and D. Wright, (2011) Biological applications of gold nanorods, *Wiley Interdiscip Rev Nanomed Nanobiotechnol* ,3, pp.100-109.

[3]. H. Huang, C. He, Y. Zeng et al., (2008) Preparation and optical properties of worm-like gold nanorods, *J Colloid Interface Sci.*, 322, pp.136-142.

[4]. . H.C. Huang, K. Rege and J.J. Heys, (2010) Spatiotemporal temperature distribution and cancer cell death in response to extracellular hyperthermia induced by gold nanorods, *ACS. Nano.,* 4, 2892-2900.

[5]. A. Gole and C.J. Murphy, (2008) Azide-derivatized gold nanorods: functional materials for "click" chemistry, *Langmuir*, 24, pp.266-272.

[6]. C.J. Murphy, T.K. San, A.M. Gole, C.J. Orendorɤ, J.X. Gao, L. Gou, S.E. Hunyadi and T. Li, (2005) Anisotropic metal nanoparticles: synthesis, assembly, and optical applications, *J. Phys. Chem. B*, 109, pp.13857-13870.

[7]. J. Alper, M. Crespo and K. Hamad-Schiɤerli, (2009) Release mechanism of octadecyl rhodamine B chloride from Au nanorods by ultrafast laser pulses, *J. Phys. Chem. C*, 113, pp.5967-5973.

[8]. T.S. Hauck, A.A. Ghazani and W.C.W. Chan, (2008) Assessing the effect of surface chemistry on gold nanorod uptake, toxicity, and gene expression in mammalian cells, *Small*, 4, pp.153-159.

[9]. G. von Maltzahn, J.H. Park, A. Agrawal, N.K. Bandaru, S.K. Das, M.J. Sailor and S.N. Bhatia, (2009) Computationally guided photothermal tumor therapy using long-circulating gold nanorod antennas, *Cancer Res.*, 69, pp.3892-3900.

[10]. G.B. Braun et al, (2009) Laser-activated gene silencing via gold nanoshell-siRNA conjugates, *ACS Nano*., 3, pp.2007-2015.

[11]. J.Y. Huang, K.S. Jackson and C.J. Murphy, (2012) Polyelectrolyte wrapping layers control rates of photothermal molecular release from gold nanorods, *Nano. Lett.*, 12, pp.2982-2987.

[12]. T.B. Huff, L. Tong, Y. Zhao, M.N. Hansen, J.X. Cheng and A. Wei, (2007) Hyperthermic effects of gold nanorods on tumor cells, *Nanomedicine UK*, 2, pp.125-132.

[13]. Z.M. Li, P. Huang et al, (2010) RGD- conjugated dendrimer-modified gold nanorods for in vivo tumor targeting and photothermal therapy, *Mol. Pharm.*, 7, pp.94-104.

[14]. P. K. Jain, I. H. El-Sayed and M. El-Sayed, (2007) Au nanoparticles target cancer , *Nano Today*, 2, pp.18-29.

[15]. Z. H. Nie, D. Fava, E. Kumacheva, S. Zou, G. C. Walker and M. Rubinstein, (2007) Self-assembly of metal–polymer analogues of amphiphilic triblock copolymers, *Nat. Mater*, 6, pp.609-614.

[16]. N. Zhao, K. Liu, J. Greener, Z. H. Nie, E. Kumacheva, (2009) Close-Packed Superlattices of Side-by-Side Assembled Au-CdSe Nanorods, *Nano Lett.*, 8, pp.3077-3081.

[17]. D. Baranov, A. Fiore, M. van Huis, C. Giannini, A. Falqui, U. Lafont, H. Zandbergen, M. Zanella, R. Cingolani and L. Manna, (2010) Assembly of colloidal semiconductor nanorods in solution by depletion attraction, *Nano Lett.*,10, pp.743–749.

[18]. Y. Mao, M.E. Cates and H.N.W. Lekkerkerker, (1995) Depletion force in colloidal systems, *Physica A*, 222, pp.10–24.

[19]. S. Underwood and P.Mulvaney, (1994) Effect of the Solution Refractive Index on the Color of Gold Colloids, *Langmuir*, 10, pp.3427-3430.

[20]. S. Link and M.A. El-Sayed, (1999) Spectral Properties and Relaxation Dynamics of Surface Plasmon Electronic Oscillations in Gold and Silver Nanodots and Nanorods, *J. Phys. Chem. B*, 103, pp.8410-8426.

[21]. S. Link and M.A. El-Sayed, (2000) Shape and size dependence of radiative, non-radiative and photothermal properties of gold nanocrystals, *Int. ReV. Phys. Chem.*, 19, pp.409-453.

[22]. C.F. Bohren and D.R. Huffman, Absorption and Scattering of Light by Small Particles; *John-Wiley: New York*, (1983).

[23]. C. Sonnichsen, T. Franzl, T. Wilk, G. von Plessen, J. Feldmann, O. Wilson and P. Mulvaney, (2002) Drastic Reduction of Plasmon Damping in Gold Nanorods, *Phys. ReV. Lett.*, 88, pp.77402(1-4).

[24]. F. Hubenthal, T. Ziegler, C. Hendrich, M.Alschinger and F. Trager, (2005) Tuning the surface plasmon resonance by preparation of gold-core/silver-shell and alloy nanoparticles, *Eur. Phys. J. D*, 34, pp.165-168.

[25]. S.J. Oldenburg, R.D. Averitt, S.L. Westcott, N.J. Halas, (1998) Nanoengineering of optical resonances, *Chem. Phys. Lett.*, 288, pp.243-247.

[26]. S. Maier, P. G. Kik and H.A. Atwater, (2002) Observation of coupled plasmon-polariton modes in Au nanoparticle chain waveguides of different lengths: Estimation of waveguide loss, *Appl. Phys. Lett.*, 81, pp.1714-1716.

[27]. N. Félidj et al, (2004) Gold particle interaction in regular arrays probed by surface enhanced Raman scattering, *J. Chem. Phys.*, 120, 7141-7146.

[28]. G. Mie, (1908) contributions to the optics of diffuse media, especially colloid metal solutions, *Ann. Phys. (Leipzig)*, 25, pp.377-445.

[29]. B.T. Draine and P.J.J. Flatau, (1994) Discrete-dipole approximation for periodic targets: theory and tests *Opt. Soc. Am. A*, 11, pp.1491-1499.

[30]. A. Akouibaa, M. Benhamou et al, (2012) numerical study of the plasmonic resonance of multi-phases nanoparticles, *Inter. Jou. Aca. Res.*, 4. No. 6, 213-223.

[31]. A. Akouibaa, M. Benhamou and A. Derouiche, (2013) Simulation of the Optical Properties of Gold Nanorods : Comparison to Experiment, *IJARCSSE,* 3 (9), 657-271.

[32]. K.L. Kelly, E. Coronado, L.L. Zhao and G.C. Schatz, (2003) The Optical Properties of Metal Nanoparticles: The Influence of Size, Shape, and Dielectric Environment, *J. Phys. Chem. B*, 107, pp.668-677.

[33]. K. S. Lee, M. A. El-Sayed, (2005) Dependence of the Enhanced Optical Scattering Efficiency Relative to That of Absorption for Gold Metal Nanorods on Aspect Ratio, Size, End-Cap Shape, and Medium Refractive Index, *J. Phys. Chem. B*, 109, pp.20331-20338.

[34]. A.C. Templeton, W.P. Wuel.ng and R.W. Murray, (2000) Monolayer-protected cluster molecules, *Acc. Chem. Res.*, 33, pp.27-36.

[35]. F. Caruso, (2001) Nanoengineering of Particle Surfaces, *Adv. Mater.*, 13, pp.1-11.
[36]. J.J. Schneider, (2001) Magnetic Core/Shell and Quantum-Confined Semiconductor Nanoparticles via Chimie Douce Organometallic Synthesis, *Adv. Mater.*, 13, 529-536.
[37]. C.J. Kiely, J. Fink, J.G. Zheng, M. Brust, D. Bethell and D.J. Schiffrin, (2000) Synthesis of thiol-derivatised gold nanoparticles in a two-phase Liquid–Liquid system, *Adv. Mater.*, 12, pp.801-802.
[38]. C.A. Mirkin, R.L. Letsinger, R.C. Mucic and J.J. Storhoff, (1996) A DNA-based method for rationally assembling nanoparticles into macroscopic materials, *Nature*, 382, 607-613.
[39]. K.H. Lee et al, (2011) Implementation of the FDTD method based on lorentz-drude dispersive model on GPU for plasmonics applications, *Prog. In Elect. Res.*, 116, 441-456.
[40]. A. Shahmansouri, and B. Rashidian, (2012) GPU Implementation of Split-Field Finite-Difference Time-Domail Method for Drude-Lorentz Dispersive Media, *Prog. In Elect. Res.*, 125, pp.55-77.
[41]. P. G. Etchegoin, E. C. Le Ru, and M. Meyer, (2006) An analytic model for the optical properties of gold, *J. Chem. Phys.*, 125 No. 16, pp.164705-3.
[42]. J.L. Young, and R.O. Nelson, (2001) A summary and systematic analysis of FDTD algorithms for linearly dispersive media, *IEEE Antennas Propag. Mag.*, 43 No. 1, 61-77.
[43]. P. G. Etchegoin, , E. C. Le Ru, and M. Meyer, (2007) Erratum: `An analytic model for the optical properties of gold, *J. Chem. Phys.*, 127 No. 18 , 189901.
[44]. A. Vial, and T. Laroche, (2008) Comparison of gold and silver dispersion laws suitable for FDTD simulations, *Appl. Phys. B*, 93, No. 1, 139-143.
[45]. V. Myroshnychenko and C. Brosseau, (2005) Finite-element method for calculation of the effective permittivity of random inhomogeneous media, *Phys. Rev. E*, 7, pp.016701-016716.
[46]. N. Jebbor and S. Bri, (2012) Effective permittivity of periodic materials: Numerical modeling by the finite element method, *J. of Electrostatics*, 70, pp.393-399.
[47]. B. Sareni, L Krähenbühl, A. Beroual, and C. Brosseau, (1996) Effective dielectric constant of periodic composite materials, *J. Appl. Phys.*, 80(3), 1688-1696.
[48]. K. Ghosh and M. E. Azimi, (1994) Numerical calculation of effective permittivity of lossless dielectric mixture using Boundary Integral Method, *IEEE Trans. on Diel. and Elect. Insul*, 1, pp.975-981.
[49]. J.N. Reddy, An Introduction to Finite Element Method, 2nd., *Mc Graw Hill, New York*, (1993).
[50]. G. Weick, R.A. Molina, D. Weinmann and R.A. Jalabert, (2005) Lifetime of the first and second collective excitations in metallic nanoparticles, *Phys. Rev. B*, 72, 115410 (1-17).
[51]. E.D. Palik, Handbook of Optical Constants of Solids III, *Academic Press, New York*, (1991).
[52]. J. Pérez-Juste, I. Pastoriza-Santos, L.M. Liz-Marzán and P. Mulvaney, (2005) Gold Nanorods: Synthesis, Characterization and Applications, *Coord. Chem. Rev.*, 249, pp.1870-1901.
[53]. S. Link and M. A. El-Sayed, (1999) Spectral Properties and Relaxation Dynamics of Surface Plasmon Electronic Oscillations in Gold and Silver Nanodots and Nanorods, *J. Phys. Chem. B,* 103, pp.8410-8426.
[54]. N.R. Jana, L. Gearheart and C.J. Murphy, (2001) Wet Chemical Synthesis of High Aspect Ratio Cylindrical Gold Nanorods, *J. Phys. Chem. B*, 105, 4065-4067.
[55]. J. Pérez-Juste et al, (2004) Electric-Field-Directed Growth of Gold Nanorods in Aqueous Surfactant Solutions, *Adv. Funct. Mater*, 14, 571-579.
[56]. A. Akouibaa, A. Derouiche and H. Redouane, (2014) Numerical study of the effects of polymeric shell on plasmonic resonance of gold nanorods, *Inter. Jou. of Com. Mater. Sci. and Eng.*, 3 (4), pp.1450024(1-19).